ORIGINAL ARTICLE

Investigation of rice husk semi-continuous combustion in suspension furnace to produce amorphous silica in ash

Soen Steven[1] · Pasymi Pasymi[2] · Pandit Hernowo[3] · Elvi Restiawaty[4] · Yazid Bindar[1,4]

Abstract

The usage of biomass can reduce vast amounts of fossil resource dependence. Rice husk is attractive due to its calorific value and high silica content in ash. In order to produce amorphous silica in ash, rice husk was combusted with temperatures below 700°C and this can be realized in a suitable furnace type, i.e. suspension furnace. This study began with rice husk ignition test in a fixed bed furnace. The ignition temperature was observed above (428 ± 8)°C. Combustion was then performed in a suspension furnace. Rice husk was semi-continuously fed when it attained the ignition temperature with total air to biomass ratio of 8.5. The mass flowrates of rice husk were set at 9.27, 20.23, 25.20, 31.36, and 42.51 kg/h. The feeding was stopped until it reached 2500 g for the first 4 variations and 500 g for the last variation. From this study, the flaming combustion lasted for 15–30 min and then continued with glowing combustion which plays an important role in the successful conversion to ash. The highest temperatures of combustion were 552–560°C. Besides, the yield of produced ash was 18.94–23.68%-wt with silica content therein of 88.29–89.15%-wt. Ash was acquired in the amorphous silica phase with unburnt carbon content of 5.11–23.27%-wt.

Keywords Combustion · Rice husk · Flame · Ash · Amorphous

1 Introduction

Biomass utilization has merits to reduce the tremendous exploitation of fossil resources in fulfilling energy and/or chemical demands [1–5]. It turns out that rice husk, as an agricultural biomass, is interesting to be valorized for its significant calorific value, and at the same time, it has rich silica content in ash [6–8]. Rice husk has calorific value which ranges from 13–17 MJ/kg [9–11], occupies up to 25%-wt of ash content [12], and contains 82.8–98.3%-wt of silica in its ash [13, 14]. Fortunately, it is widely found in developing countries but is still low in utilization [15–17].

The valorization route is through rice husk combustion and then followed by rice husk ash extraction to produce amorphous silica [18–20]. To convert rice husk ash into amorphous silica, rice husk combustion should be maintained at a maximum of 700°C. The ash then goes through a series of sol–gel processes which include acid washing of ash to remove alkaline impurities, ash extraction with alkaline solvent, precipitation of the extract with acid, gel formation and aging, gel washing, and product drying [12–14]. The final product is white color.

Amorphous silica has a wide application for adsorbent, silica gel, catalyst support, and electronics purposes [21, 22]. In contrast, if the combustion temperature surpasses 700°C, it is believed to transform the silica in ash from amorphous to crystalline phase [23–25]. Even though crystalline silica is used for building or cement mixtures, long exposure to it threatens health which can cause silicosis in human lungs [13, 20]. Therefore, the formation of crystalline silica should be suppressed.

Various studies related to rice husk combustion mainly disclosed the provision of appropriate furnaces to create

✉ Yazid Bindar
  ybybyb@itb.ac.id

1 Biomass Technology Workshop, Faculty of Industrial Technology, Institut Teknologi Bandung, Sumedang 45363, Indonesia

2 Department of Chemical Engineering, Universitas Bung Hatta, Padang 25133, Indonesia

3 Department of Chemical Engineering, Institut Sains dan Teknologi Al-Kamal, Jakarta Barat 11520, Indonesia

4 Department of Chemical Engineering, Faculty of Industrial Technology, Institut Teknologi Bandung, Sumedang 45363, Indonesia

uniform and intense mixing between raw material and combustion air [1, 26–28]. Nowadays, three types of furnaces are widely utilized to execute rice husk combustion, i.e. fixed/grated bed, fluidized bed, and suspension [29–33]. Fixed bed furnace is the oldest technology and the most frequently utilized for combustion purposes, but it has disadvantages such as long time processes, poor heat distribution which leads to hotspots generation, intense NO_X emissions, tends to ash melting due to high and non-uniform temperature, and requires extra equipment to create uniform air-material mixing [1, 29, 30, 34].

In order to achieve perfect air-material contact and offer versatility, fluidized bed furnace is the most favorable [26, 31, 35–37]. The study on co-combustion of rice husk pellet and moisturized rice husk by Ninduangdee and Kuprianov used a fluidized bed furnace with fuel staging technique and various excess air to suppress emission. However, this study only communicated combustion efficiency and emission amount where produced ash characteristics still did not become their focus. Also, the lowest combustion temperature exceeded 780 °C which can transform silica phase in ash into crystalline [32].

Likewise, a rectangular fluidized bed furnace was employed by Chokphoemphun et al. in studying the effects of excess air on rice husk combustion to gain high combustion efficiency, perfect temperature distribution, and low gas emissions [35]. Although they have succeeded in meeting the aims and objectives of their study, the temperature in the combustion chamber ranged from 789–861 °C which still has high possibility of transforming silica in ash to crystalline phase. In the meantime, the characterization of produced ash was still not examined. Other than that, the rice husk bubbling fluidized bed combustion to synthesize silica by Gomes et al. still yielded ash with crystalline silica due to contamination of bed material [36].

Martínez et al. investigated rice husk combustion study in a fluidized bed furnace with 0.15 Nm/s of air velocity and excess air of 40%-vol. The monitored temperature was nearly 760°C and the silica in ash was crystalline with 2.3%-wt of unburnt carbon content. In contrast, excess air of 125% resulted in fully amorphous silica in rice husk ash but the temperature was only at approximately 540°C and still had 7%-wt of unburnt carbon content [38].

As previously mentioned, many studies deal with rice husk combustion in fixed or fluidized bed furnaces. This kind of combustion is aimed to have high combustion efficiency for achieving maximum energy production while the characteristics of ash products still do not become a concern. If there are any, most of the ash is obtained in crystalline phase due to long exposure to high temperature or bed material contamination. Thus, the solution for rice husk combustion to produce amorphous silica in the maximum mode is by maintaining combustion temperature not exceeding 700°C [29, 30] and this can be realized by using suspension furnace.

Other advantages of suspension furnace are no need for bed material, ash can be obtained without contamination, easier to upscale, and provide lower combustion temperature than fluidized bed furnace [1, 29, 39]. Unfortunately, studies on rice husk semi-continuous combustion in suspension furnace for producing amorphous silica in ash are still lacking. There is a rice husk combustion study in this type of furnace but only focused on ash characterization in terms of crystallinity, mineral composition, morphology, and color appearance [30]. Detailed information on furnace geometry, operating conditions, multiphase flow patterns, combustion temperature, and other phenomena inside the furnace has not been provided yet.

Hence, filling the gaps and enriching the complete understanding of rice husk semi-continuous combustion in suspension furnace become the main impact of this study. It is embodied by investigating multiphase flow patterns inside the furnace, duration of flaming combustion, combustion temperature, escaped particle amount, and produced ash yield. Moreover, unburnt carbon content, crystallinity, color appearance, and mineral content in ash are also characterized and analyzed.

This study begins with the rice husk ignition test to provide information about ignition temperature for furnace start-up [38]. The combustion used rice husk as biomass and rice husk char as fuel for start-up processes. Subsequently, the performance of rice husk semi-continuous combustion and the discussion of ash characteristics are comprehensively served. The limitations of operation in this furnace as well as their follow-up to overcome finally revealed in the last section of this study.

2 Materials and methods

2.1 Materials

Rice husk was purchased in Mekarjaya rice milling at Majalaya, Bandung, Indonesia. On the other hand, rice husk char was acquired from Biomass Technology Workshop, Institut Teknologi Bandung, Indonesia. The physicochemical properties of both rice husk and rice husk char were examined through proximate analysis. Meanwhile, diesel oil for aiding initial ignition was procured from the fuel station of Pertamina (State Oil and Gas Mining Company).

2.2 Rice husk ignition test

Rice husk ignition test was held in the equipment as seen in Figure S.1a. The dimensions were 500 mm in diameter, 300 mm in height, and 100 mm in thickness. It was

equipped with temperature control and display systems (Figure S.1b). The ignition test equipment material was made from castable refractory and contained fixed bed furnace therein which was made from stainless steel with dimensions of 100 mm in diameter, 300 mm in height, and 3 mm in thickness. There was also an electric heater element in the area between castable refractory and furnace as depicted in Figure S.1c.

To avoid excessive heat loss to the environment, the equipment was covered with a castable lid. It had a feeding hole as presented in Figure S.1d. As much as 1 g of rice husk was fed into the equipment through the feeding hole and the test was carried out at 300–535°C. Afterward, the duration between rice husk feeding and the flame generation was monitored as ignition time.

2.3 Geometry of suspension furnace

2.3.1 Furnace design basis and philosophy

The suspension furnace was newly designed and fabricated. Actually, several preliminary studies regarding its geometry have been published before. The milestones from the first proposed furnace until the used furnace in this study were revealed. The 1st study investigated the effects of declination angle of tangential and secondary air pipes in the suspension furnace with two axial pipes. From the 1st study, the suitable furnace geometry was proposed to elongate particle path length, prolong particle residence time, signify turbulence effect, create recirculation flow, and produce intense swirl flow [40].

The 2nd study was more focused on visualizing and digitalizing the air and rice husk flow structures inside the suspension furnace with two axial pipes. Likewise, the influence of particle sphericity, particle diameter, feed loading rates, sinking feed inlet pipe, and temperature on escaped particle amount were reported. The 2nd study leads to understanding the appropriate technique for supplying air and rice husk to the furnace [41].

Afterward, both simulation studies were validated by the 3rd study which dealt with cold test experiments of air and rice husk flow in the suspension furnace with two axial pipes. The swirl and recirculation flow inside the furnace was intriguingly convinced by the actual cold test results. The simulation and experimental results were all close. Still, the phenomenon of backflow inside the suspension furnace occurred and was successfully solved by changing the tangential pipe angle [42]. It is on this basis and philosophy that the geometry of the suspension furnace is justified. For this study, suspension furnace with one axial air pipe to prevent the backflow phenomenon was employed.

2.3.2 Detailed geometry for fabrication

After being convinced by cold flow simulation results, the furnace is ready for fabrication. The furnace had inner diameter of 275 mm and was insulated with castable cement with thickness of 50 mm. Consequently, the outer diameter was 375 mm. The height was 1500 mm and there was a rectangular chimney with dimensions $100 \times 100 \times 300$ mm at the top area of the furnace. The axial air pipe with diameter of 130 mm and length of 750 mm was located at 600 mm from the bottom of the furnace. Axial blower for providing axial air was laid at the end of the pipe. Hopper, which was installed at 60 mm from the axial air, was utilized to semi-continuously feed the rice husk. This hopper ended with a cylindrical feeder with a diameter of 100 mm and was sunk 50 mm into the axial air pipe.

Besides, two tangential air pipes oriented 45° to the axial air pipe at 100 mm in front of the feeder. The geometry was rectangular with a size of 60×30 mm while the length was 350 mm. The rectangular geometry of tangential air pipe was chosen because it is proven to create more intense turbulence than the cylindrical one [43]. Also, there were two secondary air pipes which were tangentially installed at 250 mm from the bottom of the furnace. The secondary air pipes were 400 mm in length, 50 mm in diameter, and oriented 75° to the furnace body.

Furthermore, there was a fuel inlet with dimensions of 100×100 mm at 210 mm from the bottom of the furnace. It was used to feed rice husk char for start-up and initial ignition until the furnace temperature reached rice husk ignition point. Before the ash was collected in the ash storage chamber, it was retained in the heat sink castable with 25 mm thickness, the same diameter as the main furnace diameter, and located at 300 mm from the bottom of the furnace. A semicircular gap of 5 mm was provided to be filled with glass wool in order to reduce the amount of heat loss. The heat sink castable was embedded with holder in such a way that it can be pulled out and pushed into the furnace.

The ash storage chamber was located below heat sink castable with a dimension of $450 \times 450 \times 400$ mm. The front part of this chamber can be closed and opened to facilitate the ash collection. The furnace was also equipped with temperature display and five thermocouples. The first thermocouple was located 100 mm from the bottom of the furnace and four others were spaced 300 mm from each other.

Prior to fabrication of this suspension furnace, cold flow simulation study was again carried out to predict the flow patterns of air and rice husk in this furnace. It is hypothesized can create two types of tangential flow. One is located in the axial air pipe area due to the tangential air supply and the other was in the secondary air area. This hypothesis is proven by Fig. 1. It can be seen that there is a swirl flow pattern at the axial air pipe and at the bottom area of the furnace

Fig. 1 Swirl flow pattern in the suspension furnace for air (**a**); rice husk (**b**); Rice husk swirl flow pattern in the axial air pipe (**c**)

(a)

(b)

(c)
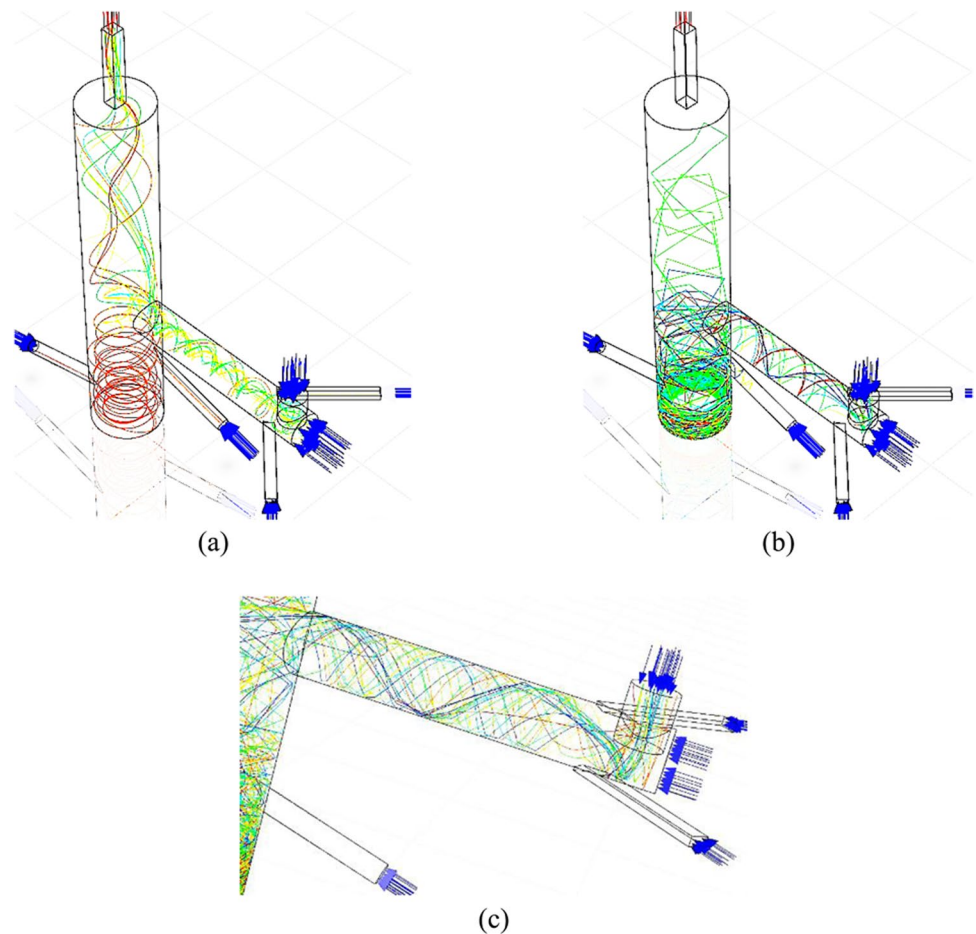
which is close to the secondary air supply because both pipes have a tangential orientation [40, 44–46]. The colors on the air flow and rice husk flow indicate multi-trajectory flow because the feed is injected using a surface type, or in other words, has more than one point [47].

The design following this geometry gives the amount of escaped particle of ± 1%. This is due to the feeder sinking as deep as 50 mm into the axial air pipe which creates vacuum effects [41]. In addition, the cold flow simulation also succeeded in proving no air and rice husk backflows out from the feeder. This proves that tangential air pipe with an orientation of 45° as well as the presence of a secondary air pipe is able to intensify the contact between air and rice husk. This intensive contact impacts the higher conversion of rice husk combustion. In fabrication stage, the top of the furnace before the chimney was equipped with cone 400 mm high. Design and fabrication of the suspension furnace are given in Fig. 2.

2.4 Furnace start-up and combustion procedure

The start-up was done by flame ignition which utilized rice husk char. The reason to use it rather than petroleum

gas is to minimize fossil fuel requirements. Rice husk char was manually fed through fuel inlet and diesel oil was then sprayed onto the char to aid initial ignition. Afterward, diesel oil was sprayed onto the rice husk char surface and the fire was ignited. The temperature at five monitored locations inside the furnace was recorded. The start-up was ended when the furnace reached rice husk ignition temperature (which was obtained from ignition test).

When the temperature achieved rice husk ignition temperature, all of the air blowers were turned on and rice husk was semi-continuously fed through the hopper and feeder. The hopper was equipped with rotating screw and feeding was held until reached the maximum capacity of furnace, 3 kg. The rice husk combustion was conducted under two conditions, i.e. at full feeding capacity (3 kg) and at 1/3 of the feeding capacity (1 kg). For all variations, 500 g of rice husk char was fed through fuel inlet. Meanwhile, rice husk was fed through feeder with the variation of screw rotations of 20 rpm, 40 rpm, 60 rpm, and 80 rpm for full feeding capacity and 100 rpm for 1/3 of feeding capacity.

Fig. 2 Design and fabrication of the suspension furnace


(a)

(b)

(c)

(d)
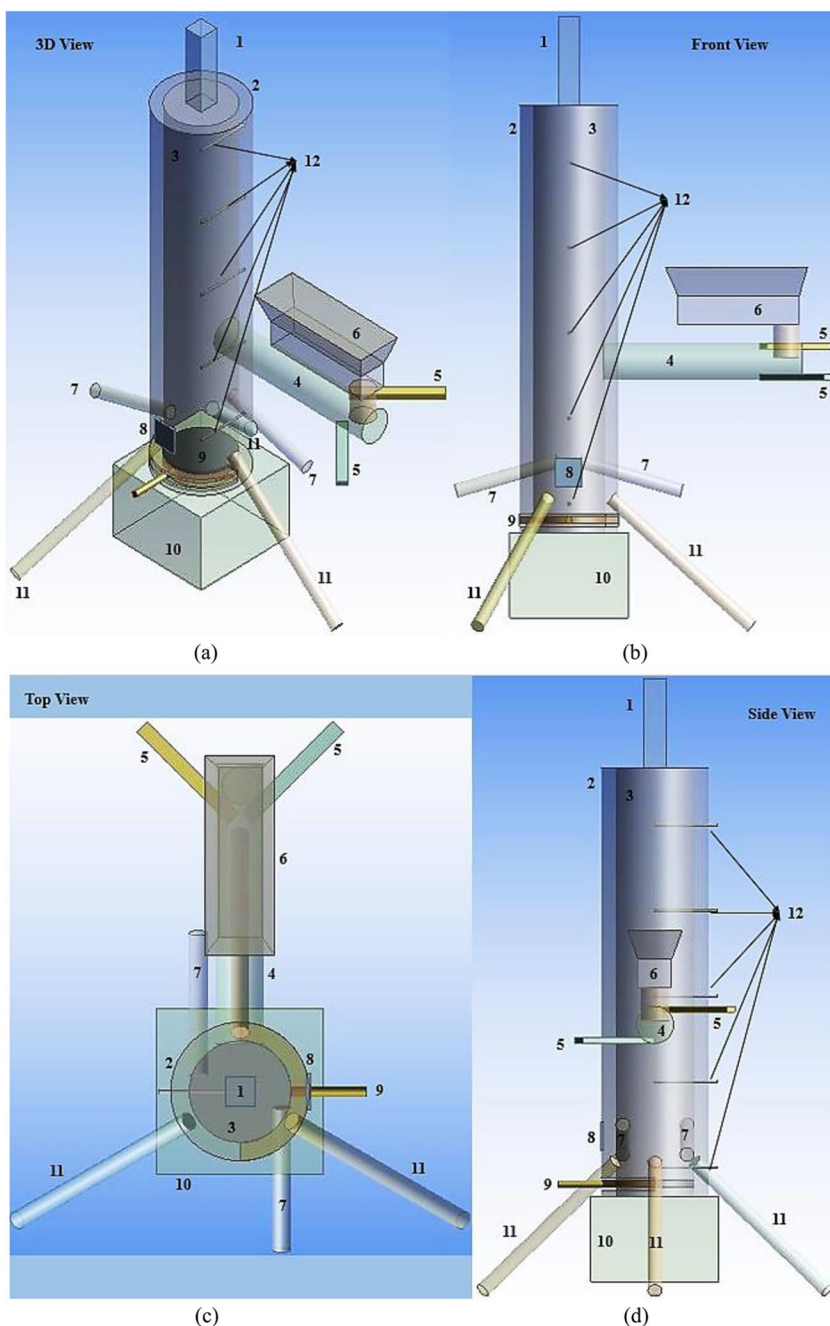
The experiment was done for 120 min and the temperature inside the furnace was recorded every 15 min. As long as the combustion takes place accompanied by the presence of flame (flaming combustion), the fuel inlet was opened and manual stirring was conducted to maintain the flame stability and ensure particle homogeneity in contact with air and fire. Manual stirring was done once every 5 min. No stirring after flaming combustion was complete and the process continued with glowing combustion for 24 h.

2.5 Analysis

The yield of ash is calculated using two definitions. First is Y_1, which represents the ratio of ash from rice husk char and rice husk itself ($m_{a,c} + m_{a,r}$) with total of rice husk char and rice husk that was fed to the furnace ($m_c + m_r$). Second is Y_2, which reflects the ratio of ash from rice husk ($m_{a,r}$) with the amount of rice husk that was fed to the furnace (m_r). The equation for calculating yield is served in Eq. (1) for the first definition and Eq. (2) for the second definition.

Fig. 2 (continued)

(e)   (f)
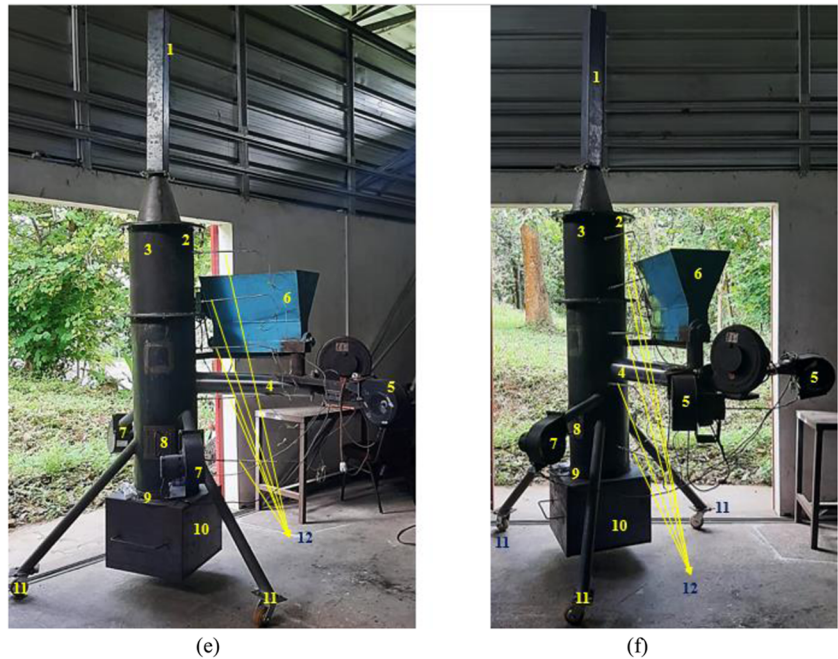
1 = Rectangular chimney (100×100×300 mm)
2 = Outer furnace body (D = 375 mm ; h = 1500 mm)
3 = Inner furnace body (D = 275 mm ; h = 1500 mm)
4 = Axial air pipe (D = 130 mm ; L = 750 mm ; h = 600 mm)
5 = Tangential air pipe (60×30×350 mm)
6 = Hopper + Feeder (L = 500 mm ; D = 100 mm, 50 mm sink into burner)
7 = Secondary air pipe (D = 50 mm ; L = 400 mm ; h = 250 mm)
8 = Fuel inlet (100×100 mm ; h = 210 mm)
9 = Heat sink castable + holder (D = 375 mm ; t = 25 mm ; h = 30 mm)
10 = Ash storage chamber (450×450×400 mm)
11 = Furnace legs + truckles
12 = Thermocouple (100 mm from bottom, +300 mm, +300 mm, +300 mm, +300 mm)

D = diameter ; L = length ; h = height ; t = thickness
(g)

$$Y_1 = \frac{m_{a,c} + m_{a,r}}{m_c + m_r} \tag{1}$$

$$Y_2 = \frac{m_{a,r}}{m_r} \tag{2}$$

The proximate analysis of rice husk, rice husk char, and rice husk ash used a thermogravimetric analyzer Apollo L. The sample was put into a crucible which is embedded in the apparatus. During operation, the sample was heated according to a predetermined program of temperature and time. The analysis was done until 900°C with a heating rate of 10°C/min. The results of moisture content, volatile matter, and ash content were recorded while the fixed carbon was acquired by difference.

Subsequently, a Bruker D8 Advance XRD instrument using Cu-Ka scanned at 2θ of 5–90° was performed to analyze ash crystallinity. The mineral content in ash was also estimated by using Rigaku ZSX Primus III + Wavelength Dispersive X-Ray Fluorescent (WD-XRF) spectrometer equipped with 50 kV and 4 mA of palladium material X-Ray generator. All samples were initially pretreated by a PVC ring pelletizer and were then dried using Myllar oven.

3 Results and discussion

3.1 Ignition test results

This study demonstrated that rice husk ignition temperature occurs at above $(428 \pm 8)^{\circ}$C or (701.15 ± 8) K. When combustion temperatures are still below ignition temperature, rice husk that has just been fed into the furnace (Fig. 3a) only decomposes to form volatile matter which is characterized
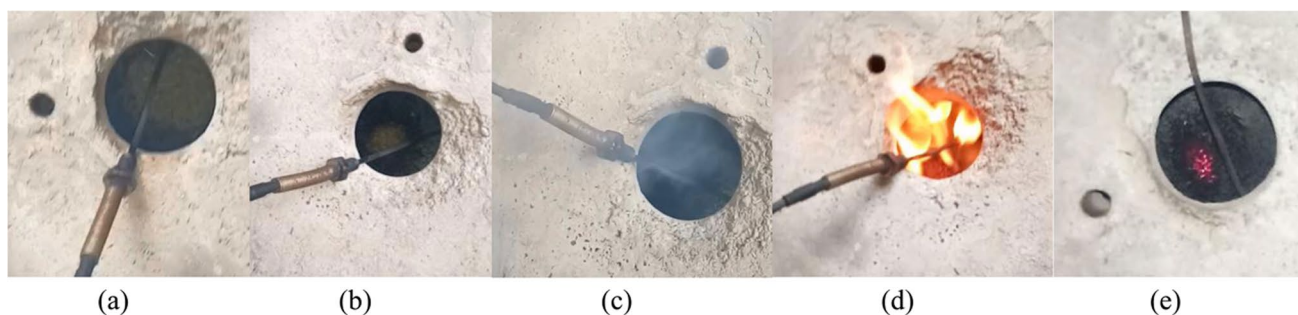
Fig. 3 Rice husk ignition phenomena: Rice husk that has just been fed into the furnace (**a**); Volatile matter decomposition (**b**); Smoke formation from devolatilization (**c**); Flaming combustion (**d**); Glowing combustion (**e**)

by smoke forming (Figs. 3b-c). At this temperature, the available energy is not enough to form flame because the volatile matter is not reactive enough to react with air [48]. Combustion only occurs between the solid surface of the rice husk and air, not accompanied by the formation of flames or known as glowing combustion [1, 49, 50] as in Fig. 3e.

In contrast, at temperatures above ignition temperature, the energy supplied by the combustion process has exceeded the devolatilization activation energy so that the reaction between the volatile matter and air can occur [51]. In this condition, combustion is characterized by flame formation as shown in Fig. 3d, so it is often called flaming combustion [48, 49, 52]. The process of flame ignition is also accompanied by a small popping sound. After the flame extinguishes, combustion continues with glow (Fig. 3e) [1].

This study also examines the rice husk ignition time. At temperatures higher than $(428 \pm 8)^{\circ}$C, the ignition time exponentially accelerates as plotted in Fig. 4a. A similar pattern was found in Jones et al. [52], but the ignition temperature and ignition time are longer because they use

pine biomass which has higher carbon and lignin contents [22, 50]. The decreasing pattern of ignition time at higher combustion temperature is also obtained from research by Pasymi using *Miscanthus giganteus* but with a shorter ignition time than rice husk because the lignin content is lesser than rice husk, 5–9%-wt vs. 25–30%-wt [24, 53–55].

The quantitative relation between ignition time and temperature is built by using two approaches. The 1st approach from Jones et al. reported that the reaction of rice husk ignition can be quantified by pseudo-first-order kinetic law [52]. As explained before, ignition happens because of the reaction between volatile matter and air under high temperatures which depends on the yield of volatile release during devolatilization [51]. For the 2nd approach, the kinetic model for biomass thermal decomposition should utilize yield of volatile release (Y_{VY}) basis following the derivation by Hernowo et al. [56]. Both approaches are then combined and applied to calculate the activation energy of rice husk ignition. The calculation is done by employing the pseudo-first-order kinetic model based on
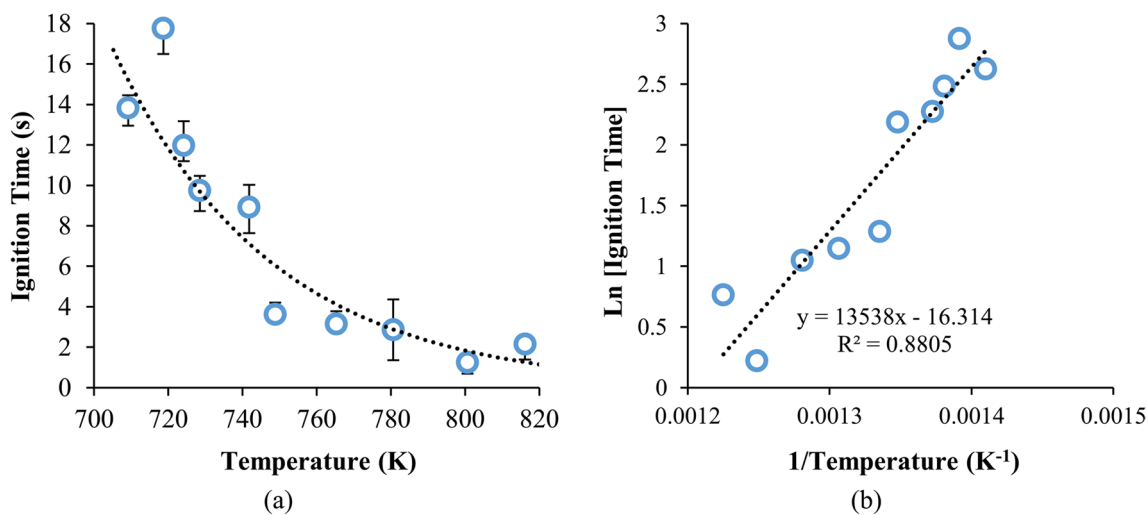
Fig. 4 Rice husk ignition time at various temperatures (**a**); Linearization plot to calculate activation energy of rice husk ignition (**b**)

Y_{VY} as in Eqs. (3a)-(3c). Rearrangement of Eq. (3c) finally produces Eq. (3e) which has the same pattern as plot of natural logarithm of ignition time vs. temperature in Jones et al. study [52].

$$\frac{dY_{VY}}{dt} = k(1 - Y_{VY}) \tag{3a}$$

$$\frac{dY_{VY}}{(1 - Y_{VY})} = kdt \tag{3b}$$

$$-ln\left(1 - Y_{VY}\right) = Aexp\left(\frac{-E_a}{RT}\right)t \tag{3c}$$

$$C = exp\left(\frac{-E_a}{RT}\right)t \tag{3d}$$

$$t = Cexp\left(\frac{E_a}{RT}\right) \tag{3e}$$

$$lnt = \frac{E_a}{RT} + lnC \tag{3f}$$

where Y_{VY} is yield of volatile release, k is kinetic constant of volatile matter release [s^{-1}], t is rice husk ignition time [s], A is Arrhenius constant [s^{-1}], E_a is activation energy of rice husk ignition [J.mol^{-1}], R is ideal gas constant [J.mol^{-1}.K^{-1}], T is fixed bed furnace temperature [K], and C is variable.

The linearization plot by means of lnt versus $\frac{1}{T}$ produces slope of $\frac{E_a}{R}$ as depicted in Fig. 4b. It plays a role in determining activation energy. From the calculation, activation energy of rice husk ignition is gained at 112.55 kJ/mol.

3.2 Air and rice husk cold flow test results

The performance of air and rice husk cold flow in the suspension furnace is reflected in the flow pattern in Fig. 5. At the bottom area of suspension furnace, the flow occurs tangentially to form a swirl as predicted by the simulation analysis in Fig. 1. Air and rice husk flow around the furnace wall as shown by the red arrows.

The rice husk mass flowrates were then determined. Rice husk was semi-continuously fed to the hopper at various screw rotations of 20 rpm, 40 rpm, 60 rpm, 80 rpm, and 100 rpm. The ratio of total air to biomass used is 8.5. The interval when the rice husk started to be fed and when all the rice husk fell to the bottom of the furnace was recorded. This experiment was carried out with 4 replicates and the results are plotted in Fig. 6.

As described before, the optimal air flow rate used is equivalent to air to biomass ratio of 8.5. In this condition, the
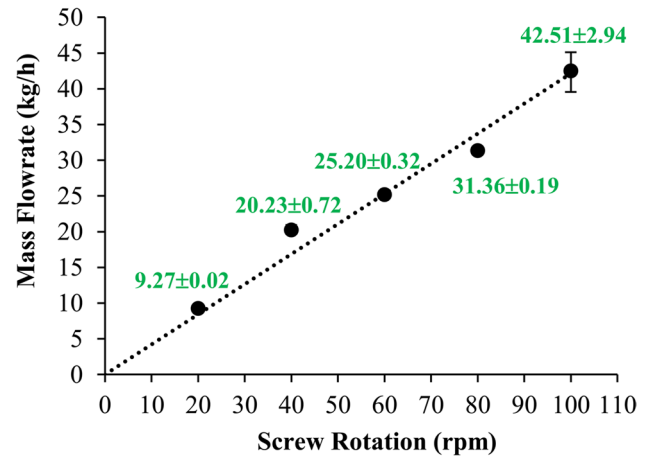

Fig. 6 Rice husk mass flowrate under various screw rotations

Fig. 5 Air and rice husk swirl flow pattern at the bottom area of suspension furnace (Red arrow indicates flow direction of rice husk)

average amount of escaped particles out from the chimney is $(1.32 \pm 0.30)\%$. This is quite similar to the predicted amount of escaped particles from the simulation. When using the ratio of 16, the number of escaped particles from the furnace increased to 14.85% (compared to the simulation from Steven et al. is 11.06% [42]).

Subsequently, the ratio was also studied at 3.9 and the flame extinguishes faster because it only last 4–8 min. The glowing combustion is finally not generated even though no particles escape. This strengthens that air flowrate should not be too low or too high because it can reduce the intensity of air-particle contact and shorten the air-particle contact time [57, 58].

3.3 Rice husk semi-continuous combustion performance

Since the total amount of rice husk was 2.5 kg, the feeding durations for 20 rpm, 40 rpm, 60 rpm, and 80 rpm are calculated at 20.7 min, 9.5 min, 7.6 min, and 6.1 min, respectively. For 100 rpm, only 500 g of rice husk was fed and required duration of 1.5 min. The rice husk combustion phenomenon inside the furnace shows flame with a swirl flow pattern as captured in Figs. 7a-c. It happens because of the secondary airflow that is tangentially supplied from the bottom area of the furnace [44–46]. Over time, the flame will slowly extinguish and begin the phase of glowing combustion [1] as indicated by red glow in Fig. 7d.

The temperature profiles in the suspension furnace during combustion are presented in Fig. 8. The zone before the red line represents the ignition phase with the aid of rice husk char until the temperature reaches the rice husk ignition temperature. The zone after the red line is at 15th min which indicates that rice husk feeding has taken place. The zone after green line represents glowing combustion. Overall, the temperature profiles in the furnace from Figs. 8a-d appear to be similar because the total amount of rice husk is in similitude.

T1 rises for 15 min, then drops until 45th min, and is followed by slow enhancement until 120th min. T1 is located at the bottom of the furnace and the flame from fuel combustion (rice husk char) occurs here causing the highest temperature. Subsequently, T1 decreased since rice husk entered the furnace. The steepest decrease in T1 is nominated to 80 rpm rather than the other three variations because more amount of rice husk is fed in a shorter duration. After 45th min, the flame extinguishes and has succeeded in changing the phenomenon to glowing combustion which is characterized by a gradual escalation in T1. Flaming combustion is important to create glow while glowing combustion plays an important role in complete conversion in combustion to produce ash. When the flame extinguishes, all blowers are turned off in order to maintain the heat generated from glowing combustion still concentrated in the rice husk bed.

In the meantime, T2 measures the flame temperature that is generated from rice husk combustion. The flame from the initial ignition with rice husk char does not reach T2. Hence, T2 is lower than T1 during the first 15 min. After the rice husk has been successfully fed, T1 becomes colder and the flames form on the top layer of rice husk bed which is reflected by the highest value of T2, at 45 min. In this condition, the values of T3-T5 are also the highest. The highest temperature inside the furnace was 511 °C, 526 °C, 539 °C, and 552 °C for 20 rpm, 40 rpm, 60 rpm, and 80 rpm, successively.

After the 45th min, the flame extinguishes so T2 decreases steeply for all variations. In consequence, T3-T5 also automatically alleviate. This also reinforces the earlier explanation that glowing combustion now plays a role because T2 is lessening rapidly whereas T1 is enhancing gently. More than that, it can be seen that T3 > T4 > T5 because the measured temperature will definitely be lower at a location that is further away from the flame. Additionally, the values of T2-T5 are getting closer at 120 min due to cooling while heat only produces at T1.

Interestingly, T1 and T2 for 100 rpm (operated at 1/3 of the feeding capacity) give a slightly different pattern, as
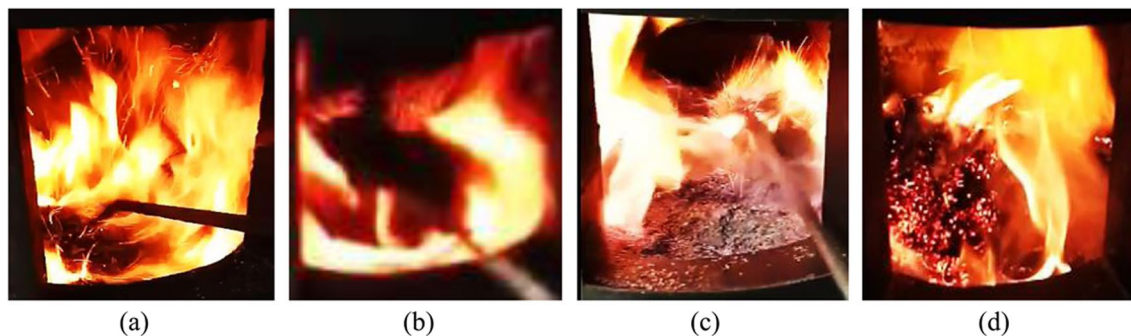

(a)   (b)   (c)   (d)

Fig. 7 Swirl flow in flaming combustion (**a-c**); Formation of glowing combustion (**d**)

Fig. 8 **a** Temperature profile in suspension furnace for rice husk feeding rate with screw rotation of 20 rpm. **b** Temperature profile in suspension furnace for rice husk feeding rate with screw rotation of 40 rpm. **c.** Temperature profile in suspension furnace for rice husk feeding rate with screw rotation of 60 rpm. **d.** Temperature profile in suspension furnace for rice husk feeding rate with screw rotation of 80 rpm. **e.** Temperature profile in suspension furnace for rice husk feeding rate with screw rotation of 100 rpm (1/3 feeding capacity)
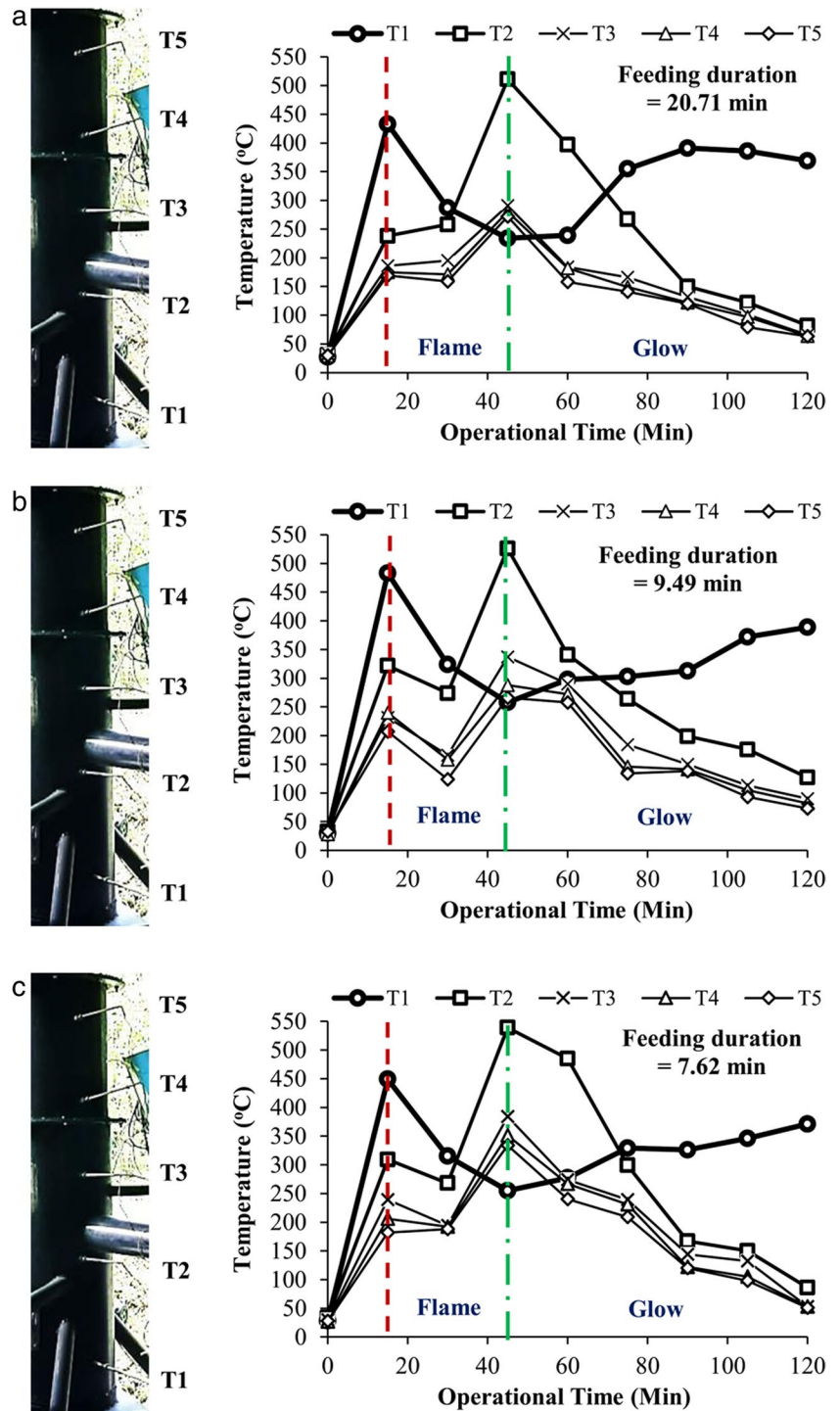
given in Fig. 9e. This is because the flame from rice husk combustion is measured only up to T1 and does not reach T2. Therefore, T1 is always higher than T2. The flame extinguishes at 30th min and then glowing combustion takes place which is indicated by gradually decremental of T1 to 462 °C at 120th min. On the other hand, T2-T5 shows a decreasing pattern after 30 min as a result of lowering furnace temperature. It can also be seen that T2 > T3 > T4 > T5 and this is rational as a result of being far away from the flame area.

At 120 min, the values of T2-T5 are also getting closer due to the cooling phenomenon and the heat is only concentrated in T1. The highest temperature in this variation is measured at 560 °C. In addition, the combustion temperature of rice husk char at the first 15 min is not identical in all
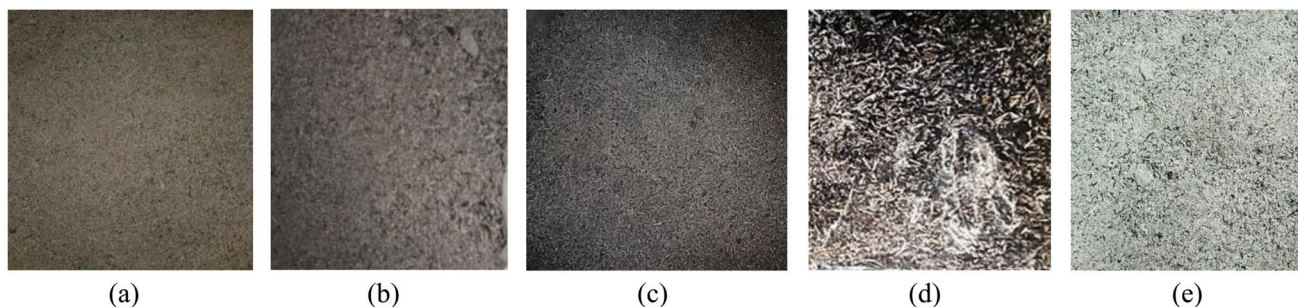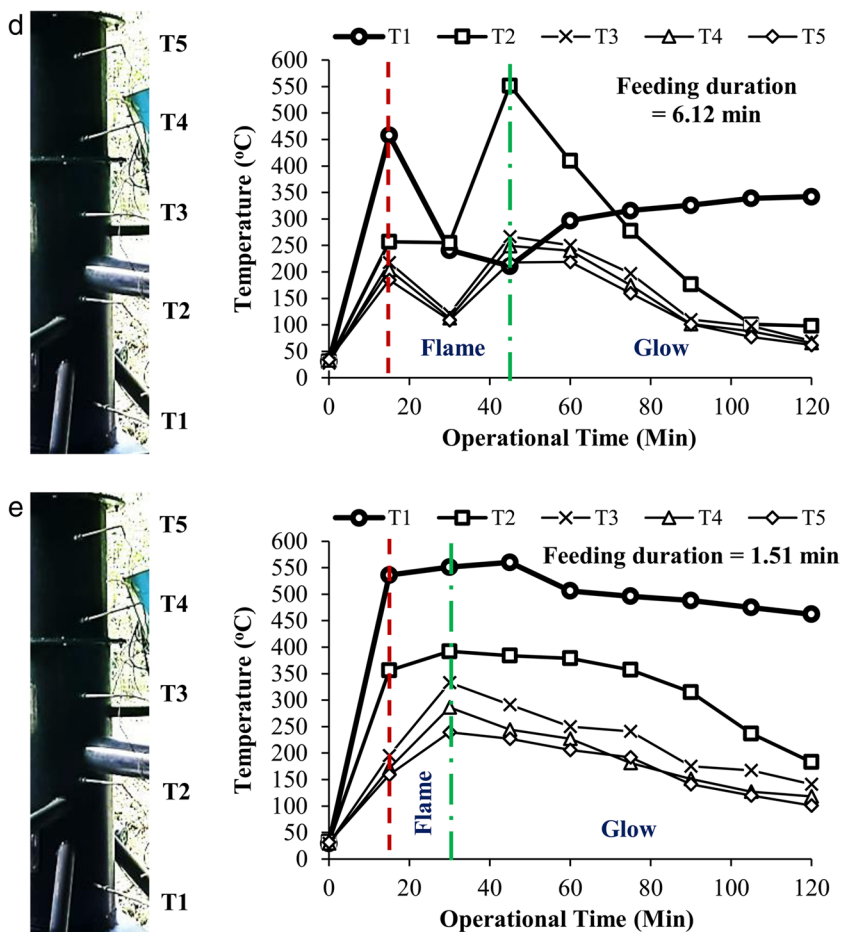
Fig. 8 (continued)

Fig. 9 The appearance of rice husk ash under rice husk feeding rates with screw rotations of 20 rpm (**a**); 40 rpm (**b**); 60 rpm (**c**); 80 rpm (**d**); and 100 rpm (**e**)

variations (433, 483, 449, 458, and 536 °C). The various values of the proximate analysis of the rice husk char samples used might be the cause of this slight temperature difference, but the deviations are still logical and close enough.

3.4 Product characteristics

As aforementioned, the success of complete rice husk combustion lies in the glowing combustion phenomenon which is allowed to stand for 24 h. This is because glowing combustion mainly deals with char combustion which becomes the rate-determining step of overall combustion rather than drying and devolatilization [39, 59]. The glowing combustion is retained for 24 h on heat sink castable which aids the heat transfer to the glowed particle. After 24 h, the resulting product is then dropped into the ash storage chamber by pulling the holder of heat sink castable. All of the appearances of the produced ash are captured in Fig. 9.

Table 1 Yield of rice husk ash under various screw rotations

| rpm	Capacity (kg)	Rice Husk Char (kg)	Rice Husk (kg)	Total Ash (kg)	Ash from Char (kg)	Y_1 (%-wt)	Y_2 (%-wt)
20	3	0.5	2.5	681.55	188.3	22.72	19.73
40	3	0.5	2.5	716.35	188.3	23.88	21.12
60	3	0.5	2.5	763.94	188.3	25.46	23.03
80	3	0.5	2.5	780.18	188.3	26.01	23.68
100	1	0.5	0.5	283.01	188.3	28.30	18.94

Table 2 Results of proximate analysis for rice husk, rice husk char, and rice husk ash

Proximate analysis	Results					
Sample	Rice husk	Rice husk char	Rice husk ash			
Screw rotation (rpm)	-	-	20	40	60	80	100
Mass flowrate (kg/h)	-	-	9.27 ± 0.02	20.23 ± 0.72	25.20 ± 0.32	31.36 ± 0.19	42.51 ± 2.94
Capacity (kg)	-	-	3	3	3	3	1
Moisture content (%-wt)	9.13	1.51	5.36	5.14	7.7	8.33	5.64
Volatile matter (%-wt)	58.31	10.31	5.98	8.68	6.5	8.35	6.58
Fixed carbon (%-wt)	12.12	50.52	10.83	14.07	18.24	23.27	5.11
Ash content (%-wt)	20.44	37.66	77.83	72.11	67.56	60.05	82.67

The product yield is outlined in Table 1. It can be seen that all of Y_1 have higher values than Y_2. This is because Y_1 calculation involves ash content in rice husk char which already occupies 37.66%-wt. In further, the ash produced from combustion results in Y_2 which is still within the range of the ash content in the rice husk itself. For a variation of 100 rpm, Y_2 has the lowest value (18.94%-wt) and represents the most complete combustion. This is also supported by the whitest ash appearance rather than the other four variations (see Fig. 9).

The unburnt carbon contents for ash from screw rotations of 20, 40, 60, 80, and 100 rpm sequentially are 10.83%-wt, 14.07%-wt, 18.24%-wt, 23.27%-wt, and 5.11%-wt as tabulated in Table 2. This implies that the combustion with the highest conversion occurs at 100 rpm, reflected by the whitest ash appearance. It happens because of the intense heat transfer between the particles and flame due to the lower feeding amount (low heat transfer resistance). Glowing combustion first occurs from the top and then propagates downwards. For the more amount of feeding rate as in the other four variations, the heat transfer resistance becomes significant and has an impact on the more unburnt carbon content in the produced ash [60]. This statement is strengthened quantitatively by higher Y_2 values in 20–80 rpm (19.73–23.68%-wt).

The fast screw rotation of 80 rpm makes more rice husk being fed in a shorter moment. This prevents rice husk from having intense contact with flame and consequently results in a high unburnt carbon content [61]. Thus, ash from 80 rpm screw rotation still has a larger value of Y_2 and black appearance. It is different from the slow screw rotation (20 rpm),
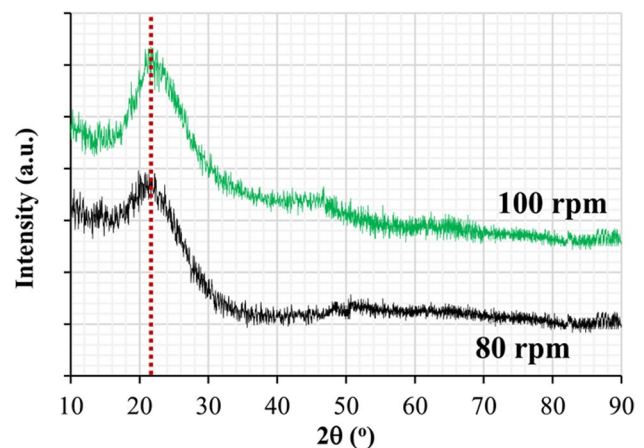
Fig. 10 Crystallinity of rice husk ash from screw rotations of 80 and 100 rpm

where rice husk is gradually fed into the furnace over a longer period of time. Rice husk finally has a greater chance of contact with flames and makes the resulting ash have a lower unburned carbon content. It is represented by lower Y_2 value and grey appearance of ash.

The crystallinity of the produced ash from 80 rpm (black appearance) and 100 rpm (the whitest appearance) are then characterized by XRD. The diffractogram in Fig. 10 informs the amorphous silica in both rice husk ash. This is because the maximum combustion temperature is at 552–560 °C which is still below the temperature that

Table 3 Mineral content in rice husk ash from screw rotations of 80 and 100 rpm

Mineral	Ash 80 rpm (%-wt)	Ash 100 rpm (%-wt)
SiO_2	89.15	88.29
Na_2O	2.71	1.40
K_2O	2.20	3.38
CaO	1.30	1.98
Cl	1.64	1.05
MgO	0.97	0.88
Al_2O_3	0.54	0.46
P_2O_5	0.61	0.69
SO_3	0.13	0.13
MnO	0.26	0.63
Fe_2O_3	0.46	1.04
ZnO	0.03	0.07

causes the transformation of the silica phase into crystalline [21, 23, 29, 36, 62–64]. The mineral content from both ashes is also examined by XRF and the results are presented in Table 3. Based on this table, the silica content in produced rice husk ash is at 88.29–89.15% -wt.

3.5 Operation study of rice husk semi-continuous combustion performance in suspension furnace

As stated in Section I, every type of combustion has its own merits and drawbacks. The limitation of fixed bed furnace can be overcome by applying fluidized bed furnace which allows perfect contact between air and fuel. Most of the studies using fluidized bed furnace have an objective to execute combustion for energy purposes because it offers high combustion efficiency and high temperature but the ash product characteristics are often overlooked. In several aspects,

drawbacks such as ash contamination with bed material and crystalline silica in ash are also frequently found. In fact, crystalline silica harms human health if often exposed for too long [13, 20].

It is clear that employing fixed bed or fluidized bed furnace hinders the aim of producing ash containing amorphous silica. The rice husk combustion in suspension furnace can be a solution for it by maintaining the temperature not exceeding 700 °C through excess air providence. Nevertheless, the potential of energy produced is sacrificed and put aside. Due to the low combustion temperature, the combustion efficiency is also poor which is implied by the attendance of unburnt carbon content in ash. For those reasons, this section attempts to communicate the gaps and technical operation study involved from the aspect of feed amount, air-to-biomass ratio, duration of flaming combustion, combustion operating time, and characteristics of the produced ash.

This suspension furnace is ideally not for lab-scale combustion or calcination because it will lead to a significant amount of unused empty space which is not feasible. However, too much rice husk amount in the suspension furnace can inhibit the heat and mass transfer between raw material and air [60, 65]. In this study, even though the capacity of 1 kg gave ash with the lowest unburnt carbon content, it is still operating below the maximum capacity. The ideal condition of air to biomass ratio to maintain the combustion temperature at 700 °C is in the range of 16–17 [59]. Other ideal condition aspects are stable flame lasting, short operating combustion time, and ash with low unburnt carbon content.

From the experiment, combustion with a capacity of 3 kg still produces ash with unburnt carbon content of 10.83–23.27%-wt. The results are still higher than Martínez et al. who obtained 2.1–12.6%-wt in fluidized bed system [38] and Gomes et al., 6.73%-wt, in suspension system [36]. This might be caused by two reasons. First is the larger rice husk mass flowrates in this study. Second, the semi-continuous combustion occurs in

Table 4 Conditions, limitations, and follow-up of the operation of this supension furnace

No	Variables	Conditions / Limitations	Follow-up
1	Rice husk feeding capacity	• Ideal condition: 3 kg rice husk combustion to produce ash with low unburnt carbon content • Actual condition: 3 kg rice husk combustion produces ash with unburnt carbon content of 10.83–23.27%-wt; 1 kg rice husk combustion produces ash with unburnt carbon content of 5.11%-wt	Choosing full feeding capacity (3 kg) with the lowest screw rotation (20 rpm) and applying the refining process in further rice husk black ash extraction
2	Air to biomass ratio	• Ideal condition: 16–17 (excess air 200%-vol) • Actual condition: 8.5 (excess air 50%-vol)	Using actual condition to alleviate the amount of escaped particles as well as to keep the flame lasting longer
3	Combustion temperature	• Ideal condition: Adiabatic, 700 °C • Actual condition: Max. 511–560 °C	It is still acceptable to use actual condition because amorphous silica in ash is the main product and energy production can not be maximal
4	Combustion operational time	• Flaming combustion: ± 30 min • Glowing combustion: ± 24 h	-

suspension mode only during feeding and at the early moment of combustion. Over time, the materials concentrate at the bottom of the furnace and the combustion is similar to fixed bed mode which has poor air-particle mixing properties.

Following this study, the amount of air supplied is at a ratio of 8.5 (lower than ideal condition). It is chosen because results in low escaped particle amount and flame is able to last for 15–30 min. If the ratio is intensified, the flame extinguishes faster and glowing combustion cannot occur. The next obstacle is difficulty of igniting rice husk so the flame is easy to extinguish and air should be supplied continuously [11]. Nevertheless, the supplied air amount also cannot be too large because it can signify the escaped particle amount.

In fact, the maximum temperature in this study is 560 °C. This impacts the longer operating time of rice husk combustion until fully converted into ash. Additionally, energy cannot be produced at maximal because of the low combustion temperature. This condition is in line with the study from Martínez et al. who call it "lean combustion" [38]. Despite the silica in ash being fully amorphous, the ash still has blackish or greyish color, known as rice husk black ash. Unfortunately, the further extraction of rice husk black ash produces silica with a black appearance. The proposed solution to overcome this is to apply the refining process by oxidation to acquire white silica products [66]. All of the conditions, limitations, and follow-up of the operation of this supension furnace are finally summarized in Table 4.

4 Conclusions

The semi-continuous rice husk combustion to produce amorphous silica in ash has been successfully studied. The furnace with a tangential air pipe angle of 45° is proven to prevent air and rice husk backflow. The secondary air pipe which is installed tangentially at the bottom area of the furnace also creates an intense swirl flow of air and rice husk. The rice husk combustion temperature should be maintained at 700°C in order to keep the silica phase in ash in an amorphous state. It can be realized by providing excess air in the combustion with the amount of 50%-vol or air to biomass ratio of 8.5. Under this condition, the flame lasted for 15–30 min, the amount of particle loss was 1.32%, and the maximal temperature was 560°C. The combustion yielded ash of 19.73–23.68%-wt with unburnt carbon content of 10.83–23.27%-wt. Moreover, the produced ash contains silica with fully amorphous phase with silica content of 88.29–89.15%-wt. Since the unburnt carbon content still remains, the refining process in rice husk ash processing to produce amorphous silica becomes a necessity. It can be done by oxidating the blackish or greyish product until turns white as common commercial silica products.

Data availability The datasets generated during and/or analyzed during the current study are available from the corresponding author upon reasonable request.

Declarations

Ethical Approval Not applicable.

References

1. Werther J, Saenger M, Hartge EU et al (2000) Combustion of agricultural residues. Prog Energy Combust Sci 26:1–27. https://doi.org/10.1016/S0360-1285(99)00005-2

2. Sharma R, Wahono J, Baral H (2018) Bamboo as an alternative bioenergy crop and powerful ally for land restoration in Indonesia. Sustain 10:1–10. https://doi.org/10.3390/su10124367

3. Quispe I, Navia R, Kahhat R (2017) Energy potential from rice husk through direct combustion and fast pyrolysis: A review. Waste Manag 59:200–210. https://doi.org/10.1016/j.wasman.2016.10.001

4. Madusari S, Jamari SS, Nordin NIAA et al (2023) Hybrid Hydrothermal Carbonization and Ultrasound Technology on Oil Palm Biomass for Hydrochar Production. ChemBioEng Rev 10:37–54. https://doi.org/10.1002/cben.202200014

5. Abdul Razak NAA, Abdulrazik A (2019) Modelling and optimization of biomass-based cogeneration plant. IOP Conf Ser: Earth Environ Sci 257:012027. https://doi.org/10.1088/1755-1315/257/1/012027

6. Bazargan A, Bazargan M, McKay G (2015) Optimization of rice husk pretreatment for energy production. Renew Energy 77:512–520. https://doi.org/10.1016/j.renene.2014.11.072

7. Su Y, Liu L, Zhang S et al (2020) A green route for pyrolysis poly-generation of typical high ash biomass, rice husk: Effects on simultaneous production of carbonic oxide-rich syngas, phenol-abundant bio-oil, high-adsorption porous carbon and amorphous silicon dioxide. Bioresour Technol 295:1–9

8. Almeida SR, Elicker C, Vieira BM et al (2019) Black SiO2 nanoparticles obtained by pyrolysis of rice husk. Dye Pigment 164:272–278. https://doi.org/10.1016/j.dyepig.2019.01.030

9. Alias N, Ibrahim N, Hamid MKA et al (2014) Thermogravimetric analysis of rice husk and coconut pulp for potential biofuel production by flash pyrolysis. Malaysian J Anal Sci 18:705–710

10. Anshar M, Ani FN, Kader AS (2014) Combustion characteristics modeling of rice husk as fuel for power plant in Indonesia. Appl Mech Mater 695:815–819. https://doi.org/10.4028/www.scientific.net/amm.695.815

11. Singh RI, Mohapatra SK, Gangacharyulu D (2011) Fluidised bed combustion and gasification of rice husk and rice straw - a state of art review. Int J Renew Energy Technol 2:345. https://doi.org/10.1504/ijret.2011.042727

12. Chakraverty A, Kaleemullah S (1991) Conversion of rice husk into amorphous silica and combustible gas. Energy Convers Manag 32:565–570. https://doi.org/10.1016/0196-8904(91)90116-Z

13. Costa JAS, Paranhos CM (2018) Systematic evaluation of amorphous silica production from rice husk ashes. J Clean Prod 192:688–697. https://doi.org/10.1016/j.jclepro.2018.05.028

14. Zarib NSM, Abdullah SA, Jamil NH (2019) Extraction of silica from rice husk via acid leaching treatment. In: The European Proceedings of Social & Behavioural Sciences. Future Academy, Asia International Multidisciplinary Conference, pp 1–6

15. Panuju DR, Mizuno K, Trisasongko BH (2013) The dynamics of rice production in Indonesia 1961–2009. J Saudi Soc Agric Sci 12:27–37. https://doi.org/10.1016/j.jssas.2012.05.002

16. FAOSTAT (2012) Food and agricultural commodities production. Food and Agriculture Organization of the United Nations Statistics, Rome, pp 1–11

17. Narvaez R, Blanchard R, Mena A (2013) Use of rice crops waste for energy production in Ecuador. Energy and Power 3:27–36. https://doi.org/10.5923/j.ep.20130303.01

18. Kalapathy U, Proctor A, Shultz J (2002) A simple method for production of silica from rice hull ash. Bioresour Technol 85:285–289. https://doi.org/10.1016/S0960-8524(02)00116-5

19. Rangaraj S, Venkatachalam R (2017) A lucrative chemical processing of bamboo leaf biomass to synthesize biocompatible amorphous silica nanoparticles of biomedical importance. Appl Nanosci 7:145–153. https://doi.org/10.1007/s13204-017-0557-z

20. Bakar RA, Yahya R, Gan SN (2016) Production of high purity amorphous silica from rice husk. Procedia Chem 19:189–195. https://doi.org/10.1016/j.proche.2016.03.092

21. Bangwar D, Saand A, Keerio M et al (2017) Development of an amorphous silica from rice husk waste. Eng Technol Appl Sci Res 7:2184–2188. https://doi.org/10.5281/zenodo.1118285

22. Prasad R, Pandey M (2012) Rice husk ash as a renewable source for the production of value added silica gel and its application: An overview. Bull Chem React Eng Catal 7:1–25. https://doi.org/10.9767/bcrec.7.1.1216.1-25

23. Azat S, Korobeinyk AV, Moustakas K, Inglezakis VJ (2019) Sustainable production of pure silica from rice husk waste in Kazakhstan. J Clean Prod 217:352–359. https://doi.org/10.1016/j.jclepro.2019.01.142

24. Azat S, Sartova Z, Bekseitova K, Askaruly K (2019) Extraction of high-purity silica from rice husk via hydrochloric acid leaching treatment. Turkish J Chem 43:1258–1269. https://doi.org/10.3906/kim-1903-53

25. Chen G, Du G, Ma W et al (2015) Production of amorphous rice husk ash in a 500 kW fluidized bed combustor. Fuel 144:214–221. https://doi.org/10.1016/j.fuel.2014.12.012

26. Nunes LJR, Matias JCO, Catalão JPS (2014) Mixed biomass pellets for thermal energy production: A review of combustion models. Appl Energy 127:135–140. https://doi.org/10.1016/j.apenergy.2014.04.042

27. Al-attab KA, Zainal ZA (2011) Design and performance of a pressurized cyclone combustor (PCC) for high and low heating value gas combustion. Appl Energy 88:1084–1095. https://doi.org/10.1016/j.apenergy.2010.10.041

28. Fang M, Yang L, Chen G et al (2004) Experimental study on rice husk combustion in a circulating fluidized bed. Fuel Process Technol 85:1273–1282. https://doi.org/10.1016/j.fuproc.2003.08.002

29. Blissett R, Sommerville R, Rowson N et al (2017) Valorisation of rice husks using a TORBED® combustion process. Fuel Process Technol 159:247–255. https://doi.org/10.1016/j.fuproc.2017.01.046

30. Fernandes IJ, Calheiro D, Kieling AG et al (2016) Characterization of rice husk ash produced using different biomass combustion techniques for energy. Fuel 165:351–359. https://doi.org/10.1016/j.fuel.2015.10.086

31. Madhiyanon T, Sathitruangsak P, Soponronnarit S (2010) Combustion characteristics of rice-husk in a short-combustion-chamber fluidized-bed combustor (SFBC). Appl Therm Eng 30:347–353. https://doi.org/10.1016/j.applthermaleng.2009.09.014

32. Ninduangdee P, Kuprianov VI (2018) Co-combustion of rice husk pellets and moisturized rice husk in a fluidized-bed combustor using fuel staging at a conventional air supply. Songklanakarin J Sci Technol 40:1081–1089. https://doi.org/10.14456/sjst-psu.2018.134

33. Kuprianov VI, Kaewklum R, Sirisomboon K et al (2010) Combustion and emission characteristics of a swirling fluidized-bed combustor burning moisturized rice husk. Appl Energy 87:2899–2906. https://doi.org/10.1016/j.apenergy.2009.09.009

34. Prasara-A J, Gheewala SH (2017) Sustainable utilization of rice husk ash from power plants: A review. J Clean Prod 167:1020–1028. https://doi.org/10.1016/j.jclepro.2016.11.042

35. Chokphoemphun S, Eiamsa-Ard S, Promvonge P, Chuwattanakul V (2019) Rice husk combustion characteristics in a rectangular fluidized-bed combustor with triple pairs of chevron-shaped discrete ribbed walls. Case Stud Therm Eng 14:100511. https://doi.org/10.1016/j.csite.2019.100511

36. Gomes GMF, Philipssen C, Bard EK et al (2016) Rice husk bubbling fluidized bed combustion for amorphous silica synthesis. J Environ Chem Eng 4:2278–2290. https://doi.org/10.1016/j.jece.2016.03.049

37. Sirisomboon K, Laowthong P (2019) Experimental investigation and prediction of heat transfer in a swirling fluidized-bed combustor. Appl Therm Eng 147:718–727. https://doi.org/10.1016/j.applthermaleng.2018.10.097

38. Martínez JD, Pineda T, López JP, Betancur M (2011) Assessment of the rice husk lean-combustion in a bubbling fluidized bed for the production of amorphous silica-rich ash. Energy 36:3846–3854. https://doi.org/10.1016/j.energy.2010.07.031

39. Ragland KW, Bryden KM (2011) Suspension burning. In: Combustion engineering, 2nd edn. CRC Press, London, pp 411–439

40. Steven S, Restiawaty E, Pasymi P, Bindar Y (2022) Three-dimensional flow modelling of air and particle in a low-density biomass combustor chamber at various declination angles of tangential and secondary air pipes. Powder Technol 410:117883. https://doi.org/10.1016/j.powtec.2022.117883

41. Steven S, Restiawaty E, Pasymi P et al (2022) Digitalized turbulent behaviors of air and rice husk flow in a vertical suspension furnace from computational fluid dynamics simulation. Asia-Pac J Chem Eng 17:e2805. https://doi.org/10.1002/apj.2805

42. Steven S, Restiawaty E, Pasymi P, Bindar Y (2022) Revealing flow structure of air and rice husk in the acrylic suspension furnace: simulation study and cold test experiment. Braz J Chem Eng 40:733–748. https://doi.org/10.1007/s43153-022-00274-y

43. Pasymi P, Budhi YW, Bindar Y (2018) Effects of tangential inlet shape and orientation angle on the fluid dynamics characteristics in a biomass burner. J Phys: Conf Ser 1090:1–8. https://doi.org/10.1088/1742-6596/1090/1/012007

44. Purwanto S, Pudjianto K, Pradana F (2018) Characteristics of powder rice husk burning on cyclone burner. Int J Sci Technol Res 7:127–130

45. Ersoy LE, Koksal M, Hamdullahpur F (1999) Effects of mode of secondary air injection on gas and solid velocity profiles in a CFB riser. In: Circulating fluidized bed technology VI. Dechema, Würzburg, pp 417–422

46. Brereton CMH, Grace JR (1993) End effects in circulating fluidized bed hydrodynamics. In: Circulating fluidized bed technology IV. Paulsboro Research Laboratory, New Jersey, pp 169–174

47. ANSYS (2019) ANSYS fluent theory guide 2019 R3. ANSYS Inc., Canonsburg

48. Rozainee M (2007) Production of amorphous silica from rice husk in fluidised bed system. Dissertation, Universiti Teknologi Malaysia

49. Stauffer E, Julia AD, Newman R (2008) CHAPTER 4 - Chemistry and physics of fire and liquid fuels. In: Fire debris analysis. Academic Press, USA, pp 85–129

50. Basu P (2013) Biomass gasification. Elsevier, pyrolysis and torrefaction. Academic Press, USA

51. Chakrabarty A, Mannan S, Cagin T (2016) Process safety. In: Multiscale modeling for process safety applications. Butterworth-Heinemann, United Kingdom, pp 32–35

52. Jones JM, Saddawi A, Dooley B et al (2015) Low temperature ignition of biomass. Fuel Process Technol 134:372–377

53. Pazla R, Jamarun N, Agustin F et al (2021) In vitro nutrient digestibility, volatile fatty acids and gas production of fermented palm fronds combined with tithonia (Tithonia diversifolia) and elephant grass (Pennisetum Purpureum). IOP Conf Ser: Earth Environ Sci 888:012067. https://doi.org/10.1088/1755-1315/888/1/012067

54. Santos EA, Silva DS, Queiroz Filho JL (2001) Composição química do capim-elefante cv. Roxo cortado em diferentes alturas. Rev Bras Zootec 30:18–23. https://doi.org/10.1590/S1516-35982001000100004

55. Pasymi P (2019) Innovation of Suspended Furnace Cyclone Burner for Combustion of Light Biomass Particles

56. Hernowo P, Steven S, Restiawaty E, Bindar Y (2022) Nature of mathematical model in lignocellulosic biomass pyrolysis process kinetic using volatile state approach. J Taiwan Inst Chem Eng 139:104520. https://doi.org/10.1016/j.jtice.2022.104520

57. Rozainee M, Ngo SP, Salema AA et al (2008) Effect of fluidising velocity on the combustion of rice husk in a bench-scale fluidised bed combustor for the production of amorphous rice husk ash. Bioresour Technol 99:703–713. https://doi.org/10.1016/j.biortech.2007.01.049

58. Rozainee M, Ngo SP, Salema AA, Tan KG (2008) Fluidized bed combustion of rice husk to produce amorphous siliceous ash. Energy Sustain Dev 12:33–42. https://doi.org/10.1016/S0973-0826(08)60417-2

59. Steven S, Hernowo P, Restiawaty E et al (2022) Thermodynamics Simulation Performance of Rice Husk Combustion with a Realistic Decomposition Approach on the Devolatilization Stage. Waste Biomass Valor 13:2735–2747. https://doi.org/10.1007/s12649-021-01657-x

60. Levenspiel O (1999) Fluid-particle reactions: kinetics. In: Chemical reaction engineering, 3rd edn. John Wiley & Sons, USA, pp 566–586

61. Rozainee M, Ngo SP, Salema AA et al (2013) Influence of bed height on the quality of rice husk ash in a fluidised bed combustor. Int J Environ Technol Manag 16:65–81

62. Adam F, Appaturi JN, Iqbal A (2012) The utilization of rice husk silica as a catalyst: Review and recent progress. Catal Today 190:2–14. https://doi.org/10.1016/j.cattod.2012.04.056

63. Jain A, Rajeswara Rao T, Sambi SS, Grover PD (1994) Energy and chemicals from rice husk. Biomass Bioenergy 7:285–289. https://doi.org/10.1016/0961-9534(94)00070-A

64. Brinker CJ, Scherer GW (1990) Sol-Gel science: the physics and chemistry of Sol-Gel processing. Academic Press, USA, pp 1–880

65. Levenspiel O (1999) Reactors with Suspended solid catalyst, fluidized reactors of various types. In: Chemical reaction engineering, 3rd edn. John Wiley & Sons, USA, pp 447–451

66. Steven S, Restiawaty E, Pasymi P, Bindar Y (2021) Influences of pretreatment, extraction variables, and post treatment on bench-scale rice husk black ash (RHBA) processing to bio-silica. Asia-Pac J Chem Eng 16:e2694. https://doi.org/10.1002/apj.2694